HHS Public Access

Author manuscript

J Trauma Acute Care Surg. Author manuscript; available in PMC 2022 June 01.

Published in final edited form as:

J Trauma Acute Care Surg. 2021 June 01; 90(6): 1022–1031. doi:10.1097/TA.0000000000003164.

Cryoprecipitate Attenuates the Endotheliopathy of Trauma in Mice Subjected to Hemorrhagic Shock and Trauma

Mark Barry, MD[1], **Alpa Trivedi, PhD**[2], **Byron Y. Miyazawa, BA**[2], **Lindsay R. Vivona, BS**[2], **Manisha Khakoo**[2], **Haoqian Zhang, PhD**[2], **Praneeti Pathipati, PhD**[2], **Anil Bagri, MD PhD**[3], **Michelle G. Gatmaitan, BS**[3], **Rosemary Kozar, MD PhD**[4], **Deborah Stein, MD MPH**[1], **Shibani Pati, MD PhD**[2,*]

[1]University of California, San Francisco. Department of Surgery. 513 Parnassus Ave. San Francisco, CA 94143

[2]University of California, San Francisco. Department of Laboratory Medicine. 513 Parnassus Ave. San Francisco, CA 94143

[3]Cerus Corporation. 1220 Concord Ave. Concord, CA

[4]Shock Trauma Center, University of Maryland School of Medicine, Baltimore, MD

Abstract

Background: Plasma has been shown to mitigate the endotheliopathy of trauma (EOT). Protection of the endothelium may be due in part to fibrinogen and other plasma-derived proteins found in cryoprecipitate, however the exact mechanisms remain unknown. Clinical trials are underway investigating early cryoprecipitate administration in trauma. In this study, we hypothesize that cryoprecipitate will inhibit endothelial cell (EC) permeability *in vitro* and will replicate the ability of plasma to attenuate pulmonary vascular permeability and inflammation induced by hemorrhagic shock and trauma (HS/T) in mice.

Methods: *In vitro*, barrier permeability of ECs subjected to thrombin challenge was measured by trans-endothelial electrical resistance. *In vivo*, using an established mouse model of HS/T, we compared pulmonary vascular permeability among mice resuscitated with 1) lactated Ringer's (LR), 2) fresh frozen plasma (FFP), or 3) cryoprecipitate. Lung tissue from the mice in all groups was analyzed for markers of vascular integrity, inflammation, and inflammatory gene expression via NanoString mRNA quantification.

Results: Cryoprecipitate attenuates EC permeability and EC junctional compromise induced by thrombin *in vitro* in a dose-dependent fashion. *In vivo*, resuscitation of HS/T mice with either FFP

*Indicates corresponding author to whom correspondence should be addressed, Shibani Pati, MD PhD, Professor, Department of Laboratory Medicine, 513 Parnassus Avenue, San Francisco, CA 94143, Shibani.pati@ucsf.edu, Phone: (713)299-0788.

Author Contributions: All authors participated in manuscript preparation. S.P. participated in the planning, execution and analysis of the experiments. M.B., S.P., A.T planned the experiments. M.B. and P.P. performed the *in vivo* experiments. L.V., P.P. and B.M. performed the in vitro assays. M.K. and H.Z. performed the histological analysis. M.B. and A.T. did statistical analyses, gene expression analysis, prepared the figures, and interpreted the data. A.B., M.G., R.K., and D.S. contributed to writing and providing the clinical relevance and input for the paper.

Conflicts of Interest: Anil Bagri and Michelle Gatmaitan are employees of Cerus Corporation. Shibani Pati had a grant from CSL Behring, unrelated to this work. The remaining authors have no conflicts of interests to disclose.

Presentation: This research is being presented at the 51st Annual Meeting of the Western Trauma Association, 2021.

or cryoprecipitate attenuates pulmonary vascular permeability (sham: 297±155, LR: 848±331, FFP: 379±275, cryoprecipitate: 405±207; $p<0.01$ sham vs. LR, $p<0.01$ LR vs. FFP, and $p<0.05$ LR vs. cryoprecipitate). Lungs from cryoprecipitate- and FFP-treated mice demonstrate decreased lung injury, decreased infiltration of neutrophils and activation of macrophages, and preserved pericyte-endothelial interaction compared to LR-treated mice. Gene analysis of lung tissue from cryoprecipitate- and FFP-treated mice demonstrates decreased inflammatory gene expression, in particular IL-1β and NLRP3, compared to LR-treated mice.

Conclusion: Our data suggest that cryoprecipitate attenuates the EOT in HS/T similar to FFP. Further investigation is warranted on active components and their mechanisms of action.

Keywords

Cryoprecipitate; fresh frozen plasma; hemorrhagic shock; endotheliopathy of trauma; acute lung injury

BACKGROUND

Traumatic injury is the leading cause of death in the United States among individuals from ages 1 to 44.(1) Damage control resuscitation, which includes early administration of balanced ratios of red blood cells, fresh frozen plasma, and platelets, has been a significant advance in trauma and critical care and has improved outcomes such as decreasing hemorrhage-related mortality.(2-6) However, hemorrhage continues to account for a substantial portion of morbidity and mortality following trauma.(7-9) While the majority of deaths in trauma occur within 24 hours after injury, an estimated 25% of deaths occur after 72 hours, most of which are attributed to inflammatory causes such as multiple organ failure, acute respiratory distress syndrome (ARDS), sepsis, and venous thromboembolic disease.(7, 8, 10) These late deaths are potentially reflective of the endotheliopathy of trauma (EOT), which refers to the combination of endothelial injury, endothelial barrier compromise, systemic inflammation, dysfunctional coagulation, and ultimately multiple organ failure that results from traumatic injury, shock, and resuscitation.(11, 12)

Traditionally plasma has been thought to exert its clinical benefits via improved hemostasis and replacement of lost blood volume, however plasma-based resuscitation has also been shown to mitigate the EOT in pre-clinical models of injury. In rodent models of hemorrhagic shock and trauma (HS/T), fresh frozen plasma (FFP) transfusion has been shown to inhibit vascular permeability and tissue edema, decrease inflammation, and reduce lung injury. (13-17) Plasma also restores the endothelial glycocalyx, a network of glycoproteins and proteoglycans on the lumenal surface of the endothelium that regulates vascular permeability and leukocyte- and platelet-endothelial cell interactions.(18-23)

One limitation of FFP is that it contains low levels of fibrinogen and is therefore inefficient in treating hypofibrinogenemia in the trauma patient. Fibrinogen is the first coagulation factor to be depleted in massive hemorrhage.(24) Among severe trauma patients, hypofibrinogenemia is common and is an independent predictor of the need for massive transfusion and death.(24-28) There is a growing body of evidence demonstrating improved outcomes with administration of fibrinogen concentrate versus FFP, which suggests that

early replacement of fibrinogen in patients with hemorrhagic shock may be advantageous.(23, 29-31)

In the United States cryoprecipitate is used to replace fibrinogen in bleeding trauma patients, however it is typically given late in massive transfusion protocols or after hypofibrinogenemia has already developed. Cryoprecipitate is prepared from plasma and contains high levels of fibrinogen, von Willebrand factor, factor VIII, and factor XIII. Two recently published small randomized controlled trials have demonstrated feasibility of early administration of fibrinogen concentrate or cryoprecipitate in trauma patients with hemorrhagic shock.(32, 33) The CRYOSTAT-2 (ISRCTN 14998314) randomized controlled trial is currently underway in the United Kingdom and is the first to evaluate the effect of early administration of high-dose cryoprecipitate versus standard therapy on mortality in trauma patients requiring massive transfusion.

Whether cryoprecipitate replicates the beneficial effects of plasma in mitigating the EOT is unknown. Recent studies have shown that fibrinogen and cryoprecipitate have protective effects on the endothelial barrier *in vitro*.(23, 34, 35) In this study we seek to further investigate the physiological and biological effects of cryoprecipitate on the EOT both *in vitro* in endothelial cells (ECs) and after early administration *in vivo* in an established mouse model of HS/T.(13, 36) We hypothesize that cryoprecipitate will attenuate injury-induced pulmonary vascular endothelial permeability *in vitro* and will replicate the ability of FFP to attenuate pulmonary vascular permeability and inflammation induced by HS/T in mice.

METHODS

Reagents

Fresh frozen plasma (FFP) was obtained from Vitalant (Denver, CO). Cryoprecipitate was obtained from Central California Blood Center (CCBC, Fresno, CA).

Quantitation of Endothelial Barrier Permeability in Vitro

Human umbilical vein endothelial cells (HUVECs) were obtained from PromoCell (Heidelberg, Germany) and maintained using Endothelial Cell Growth Medium 2 (PromoCell). The integrity of HUVEC monolayers was measured using an electric cell-substrate impedance sensing system (ECIS 1600, Applied BioPhysics, Troy, NY). HUVECs were grown to confluence on L-cysteine reduced 96-well plates containing electrodes in each well. Cells were treated with cryoprecipitate (0.25%, 2.5%, 5%, and 10%) or 10% FFP and were challenged after 30 minutes with thrombin 0.2U/ml (Sigma, St. Louis, MO). Transendothelial electrical resistance (TEER), which correlates inversely with endothelial paracellular permeability, was measured across HUVEC monolayers at 4/16/64 kHz in 8-min intervals. Data were normalized to the mean resistance of cell monolayers measured before the treatments.

Immunostaining of Endothelial Adherens Junction Proteins in Vitro

In a separate experiment, HUVECs were grown to confluence on 24-well culture plates. Cryoprecipitate (5%) or FFP (10%) was added to the HUVEC monolayer for 30 minutes,

followed by a 0.2U/ml thrombin challenge for 5 minutes at 37°C. Cells were then fixed with 4% paraformaldehyde. Adherens junctions were stained with antibodies against VE-cadherin (Cell Signaling, Danvers, MA), and f-actin was detected with Texas Red Phalloidin (Cell Signaling). Representative images were captured at 20x magnification using a Revolve microscope (Echo Inc., San Diego, CA). Gap junction measurements were performed using CellInsight CX7 LZR (Thermo Fisher, Asheville, NC).

Animals

The animal studies were performed with approval of the Institutional Animal Care and Use Committee (IACUC) at UCSF. The experiments were conducted in compliance with the ARRIVE guidelines for animal models and National Institutes of Health (NIH) guidelines on the use of laboratory animals. All animals were housed in a room with access to food and water ad libitum, controlled temperature and 12:12-hour light-dark cycles.

Hemorrhagic Shock and Trauma Mouse Model

Male C57BL6 mice, 8-12 weeks old, were obtained from The Jackson Laboratory (Sacramento, CA) (N=12-18 per group). Under inhaled isoflurane anesthesia, animals were placed on a heating plank to maintain body temperature between 35°C and 37°C. Femoral arterial catheters were flushed with 1,000-U/ml heparin and then cannulated into the femoral arteries of both legs. No additional heparin was used. The right catheter was used for continuous blood pressure monitoring (PowerLab 8, AD Instruments, Dunedin, New Zealand), and the left catheter was used for blood withdrawal and resuscitation. A 2-cm midline laparotomy was performed to induce trauma, and internal organs were inspected. Mice were then bled to a mean arterial blood pressure (MAP) of 35 mmHg for 90 minutes. (13, 36) After the 90-minute shock period, mice received low-volume resuscitation with 200 μl total of 1) lactated Ringer's (LR), 2) fresh frozen plasma (FFP), or 3) cryoprecipitate (a weight-based dose of 4.3 μl per mg of body weight plus additional LR to total 200 μl). This dose of cryoprecipitate was chosen to approximate the dose of cryoprecipitate being administered in the CRYOSTAT-2 trial (15 units) to a typical 70 kg adult. Sham mice underwent cannulation without laparotomy or blood withdrawal. Mice were monitored for an additional 30 minutes after resuscitation and were then allowed to ambulate freely for 60 minutes.

In Vivo Pulmonary Vascular Permeability

Three hours after the initiation of shock, mice were anesthetized with isoflurane and 0.2 ml of 0.2 mg/ml 10 kDa dextran conjugated with Alexa Fluor 680 was administered via the femoral cannula as previously reported.(16) 30 minutes after injection, the mice were perfused with 30 ml of ice-cold phosphate-buffered saline via the left ventricle to flush the blood from the lungs. The left lung was harvested and scanned on the Odyssey CLx Imager (LI-COR, Lincoln, NE), and the infrared signal was read at 700nm to detect the dye that had extravasated out of the vasculature into the tissue. Using Image Studio Version 5.2 (LI-COR), an average fluorescence intensity per area was quantitated for each lung.

Histologic Analysis of Lung Injury and Immunostaining of Lungs for Inflammatory Infiltrates

Lungs were post-fixed overnight in 4% PFA at 4°C and subsequently dehydrated in 30% sucrose at 4°C for 3-5 days. Lungs were embedded in OCT and stored at −80°C until they were sectioned on a Leica CM 1950 Cryostat (Wetzlar, Germany) at 10 μm thickness. Tissue sections were stained with Hematoxylin & Eosin at the Mouse Pathology Core (University of California, San Francisco). Sections were imaged with a Revolve microscope (Echo Inc., San Diego, CA). Three H&E sections from each mouse were assessed for semi-quantitative analysis of alveolar collapse, wall thickening, and inflammatory cell infiltrates. Representative images based on the lung injury score were selected from each group. Additional sections were stained with antibodies against Ly6G (Abcam, Burlingame, CA) and CD68 (BioRad, Hercules, CA).

Scoring of Histologic Lung Injury

Two sections from each mouse were assessed for alveolar damage by two blinded researchers before a representative image was selected from each group. Three or more 100X power fields per mouse were assessed by a scoring system from 1-4 to quantify pulmonary alveolar injury and lung morphological changes. A score of 1 is the least injured with less than 10% of the pulmonary area assessed demonstrating alveolar collapse or inflammatory cell infiltration. A score of 2 indicates 20-40% collapse or inflammatory cell infiltration, a score of 3 indicates 40-70% collapse or inflammatory cell infiltration, and a score of 4 indicates 70-100% collapse or inflammatory cell infiltration.(37) Wall thickening was assessed by the number of images with demonstrable thickened alveolar wall structures.

Immunostaining of Lungs for Markers of Endothelial Junctional Stability

A second cohort of animals was perfused with 10 ml of ice-cold PBS, and the left lung was flash-frozen in isopentane and stored at −80°C until they were sectioned at 10 μm thickness. Isopentane sections were fixed in ice-cold 95% EtOH for 20 minutes then 100% acetone for 1 minute. Tissue sections were stained with antibodies against VE-cadherin (R&D System, Minneapolis, MN), ZO-1 (Abcam), PDGFR-beta (Abcam), and CD31 (Millipore, Burlingame, MA). Sections were imaged with a Nikon Eclipse 80i microscope (Nikon, Melville, NY) with RT-scmos camera (SPOT Imaging, Sterling Heights, MI).

Gene Expression Analysis with NanoString nCounter

Using the second cohort of animals, gene expression in the lung was analyzed at 3 hours post-shock. Briefly, total RNA was isolated from lung lysates using the ALLPrep DNA/RNA mini kit (Qiagen, Germantown, MD) and quality control assessed with a DeNovix DS-11 Spectrophotometer (DeNovix, Wilmington, DE). Using nCounter technology from Nanostring, we then measured copy numbers of all 750 genes in the mouse nCounter® Autoimmune Profiling Panel (NanoString, Seattle, WA). N=3 mice per group (sham, cryoprecipitate, FFP) and N=6 mice (LR) were processed for gene expression.

Statistical Analysis

Data comparison of more than two groups in the *in vitro* or *in vivo* experiments were analyzed using one-way ANOVA with Tukey's post hoc tests. Mean arterial pressures were compared using repeated measures two-way ANOVA followed by Tukey's multiple comparison test. $P<0.05$ was considered significant. These analyses were performed using Prism 9.0 (Graphpad Inc., San Diego, CA). Data in this manuscript are presented as mean ± SD.

Differential gene expression was analyzed using nSolver Analysis Software 4.0 and nCounter Advanced Analysis 2.0.134 (NanoString). Samples were normalized to positive controls and housekeeping genes using the Advanced Analysis geNorm algorithm.(38) The advanced analysis module performs linear regressions to calculate differential gene expression between treatment groups with correction for multiple comparisons using the Benjamini-Yekutieli false discovery rate method.(39)

RESULTS

Cryoprecipitate attenuates thrombin-induced endothelial barrier permeability *in vitro.*

We compared the effects of cryoprecipitate and FFP to media alone on barrier permeability of HUVEC monolayers subjected to thrombin challenge. TEER tracings demonstrate that similar to FFP, cryoprecipitate attenuated endothelial barrier permeability in a dose-dependent fashion with the strongest effects at 5% cryoprecipitate (Area under the curve for thrombin: −0.57±0.04, cryoprecipitate 0.25%: 0.02±0.08, cryoprecipitate 2.5%: 0.17±0.07, cryoprecipitate 5%: 0.32±0.03, cryoprecipitate 10%: 0.13±0.04, FFP 10%: 0.63±0.06; all groups $p<0.0001$ vs. thrombin) (Figure 1A).

Cryoprecipitate attenuates thrombin-induced breakdown of endothelial adherens junctions *in vitro*.

We sought to determine if the protective effect of cryoprecipitate on endothelial barrier permeability was secondary to protection of EC adherens junctions. Untreated ECs *in vitro* are packed tightly with strong staining for VE-cadherin (green), as well as a quiescent level of F-actin (red). Following thrombin challenge, there was a loss of VE-cadherin expression and an increase in f-actin expression levels, ultimately resulting in the formation of large gaps throughout the EC monolayer. These effects were mitigated by FFP and cryoprecipitate where images denote partial preservation of VE-cadherin in ECs. Quantification of gap lengths between cells demonstrates that cryoprecipitate and FFP significantly attenuated thrombin-induced paracellular gap formation in the ECs (Figure 1B).

Cryoprecipitate and FFP are superior to LR in restoring mean arterial pressures (MAPs) and decreasing pulmonary vascular permeability in mice subjected to HS/T.

In vivo in a mouse model of HS/T, there was a significant treatment effect over time on MAPs after resuscitation as determined by repeated measures two-way ANOVA ($p<0.0001$) (Figure 1C). 30 minutes after resuscitation, both cryoprecipitate and FFP resulted in higher MAPs than LR ($p<0.0001$). Although cryoprecipitate resulted in lower MAPs at 10–15 minutes compared to FFP ($p<0.001$), the MAPs became similar at 25 minutes post-

resuscitation, and at 30 minutes MAPS were higher in the cryoprecipitate group than the FFP group ($p<0.05$).

The average fluorescence intensity of extravasated dye in the harvested lung was measured at three hours after initiation of shock (Figure 1D). HS/T resulted in increased permeability in LR-treated animals compared to sham mice (sham: 297±155, LR: 848±331, p=0.003). Both FFP and cryoprecipitate caused a dramatic attenuation of permeability compared to LR (FFP: 379±275, p=0.009; cryoprecipitate: 405±207, p=0.015). The fluorescence intensities of mice treated with FFP or cryoprecipitate were not significantly different from sham (p=0.94 and p=0.87, respectively) or each other (p=0.99) (Figure 1D).

Cryoprecipitate and FFP decrease lung injury, inflammation, and loss of vascular adherens and epithelial tight junctions in HS/T mice.

Histopathological analysis of the lungs reveals that HS/T mice treated with LR demonstrate increased levels of pulmonary alveolar injury and inflammatory cell infiltrates compared to FFP- or cryoprecipitate-treated mice (Figure 2). The percentage of images with alveolar wall thickening was 21% among sham mice, 65% among LR-treated mice, 33% among FFP-treated mice, and 8% among cryoprecipitate-treated mice. Immunofluorescent staining of the lungs for CD68, a marker of monocytes and macrophages, demonstrates activation of alveolar macrophages as evidenced by increased formation of cell membrane protrusions by the macrophages in the LR group,(40) which were decreased in the FFP and cryoprecipitate groups (Figure 3A, see arrows). Staining for the neutrophil marker Ly6G demonstrates qualitative decreases in neutrophil infiltration induced by HS/T in mice treated with FFP and cryoprecipitate compared to those treated with LR (Figure 3B).

The tight junction protein ZO-1 is a marker of both epithelial and endothelial tight junctions. ZO-1 in the epithelial-lined airways was notably compromised by HS/T. Cryoprecipitate and FFP both qualitatively attenuate the loss of epithelial ZO-1 compared to LR mice (Figure 4A). Furthermore, staining for vascular adherens junctions (VE-cadherin) demonstrates diminished breakdown in FFP- and cryoprecipitate-treated mice compared to LR-treated mice (Figure 4B). Pericytes play an important role in conferring vascular stability.(41) Our data demonstrate a loss of pericytes along the vessel wall in LR-treated HS/T mice. In contrast, FFP- and cryoprecipitate-treated mice demonstrate preserved pericyte coverage of the abluminal vessel area (Supplemental Figure 1).

Cryoprecipitate and FFP decrease the upregulation of pro-inflammatory gene expression in the lungs of HS/T mice.

To evaluate changes in gene expression early after HS/T, we analyzed total RNA extracted from lung tissue using the NanoString Mouse Autoimmune Profiling Panel of 750 genes. There were 141 genes that were significantly up- or down-regulated in HS/T mice treated with LR compared to sham mice based on an unadjusted p-value of 0.05. Figure 5A shows the $\log_2$ fold change in gene expression between HS/T mice compared to sham mice, and the top 40 most statistically significant genes are presented in Table 1A. The figure and table show that a number of pro-inflammatory genes were significantly upregulated in LR-treated HS/T mice compared to sham mice, which was attenuated by FFP and to a lesser extent

cryoprecipitate. Several of the genes involved in the innate immune system and inflammasomes—including Il-1β, NLRP3, NFKB2, CLEC4E, and CXCL10—were expressed at significantly lower levels in both the FFP and cryoprecipitate groups compared to LR, suggesting possible pathways by which FFP and cryoprecipitate mitigate HS/T-induced inflammation in the lung (Figure 5B, Table 1B).

DISCUSSION

Our previous studies show that in mice, resuscitation with FFP mitigates HS/T-induced pulmonary vascular permeability and inflammation.(13-17) Similarly, *in vitro* cryoprecipitate has protective effects on EC permeability and the EC glycocalyx.(23, 34, 35) In this study we hypothesize that cryoprecipitate will have protective effects on pulmonary injury, vascular compromise, and inflammation in an established animal model of HS/T. Cryoprecipitate does indeed recapitulate many of the effects of FFP on EC permeability and adherens junction breakdown *in vitro*. *In vivo* in a mouse model of HS/T we find that pulmonary vascular permeability and junction breakdown is attenuated by FFP and cryoprecipitate but not LR resuscitation. FFP and cryoprecipitate also attenuate inflammatory infiltration of the lung, preserve pericytes that regulate vascular stability, and decrease the expression of a number of genes associated with trauma-induced inflammation and ARDS.

Utilizing NanoString technology, we demonstrate upregulation of inflammatory genes in the lungs early after HS/T. The expression of pro-inflammatory and some anti-inflammatory genes rises significantly after injury in LR-treated mice, whereas resuscitation with FFP and to a lesser extent cryoprecipitate normalize many of these genes toward levels seen in sham animals (Figure 5). There are several notable pro-inflammatory genes whose upregulation was prevented by both FFP and cryoprecipitate, including IL-1β, NLRP3, CXCL10, TLR2, TNF, NFKB2, and CLEC4E (Table 1). The corresponding proteins for several of these genes, including NLRP3, TLR2, NF-κB, and IL-1β, are known to interact closely which each other in mediating the systemic inflammatory response to danger-associated molecular patterns (DAMPs).(42-44) These findings are concordant with studies that have shown that NLRP3 inflammasomes and Il-1β play a critical role in acute lung injury,(45) HS-induced lung injury,(46, 47) and uncontrolled inflammation in trauma.(48) Among mice resuscitated with FFP or cryoprecipitate, there was also a substantial relative decrease in gene expression for the chemokine CXCL10, which has been implicated in the development of ARDS.(49) Expression of CLEC4E, which encodes for Mincle, a C-type lectin receptor that senses cell death and induces inflammatory cytokine production and neutrophil infiltration into damaged tissue,(50) was also reduced in these groups, however its role in HS/T has not been investigated. Interestingly there were also several anti-inflammatory genes upregulated in HS/T that were decreased by FFP and cryoprecipitate compared to LR. For example, the expression of TNFAIP3, a known negative regulator of the NF-κB pathway,(51) was significantly upregulated in the LR group, but this was not seen in the FFP- or cryoprecipitate-treated mice. This suggests that there is activation of a number of pathways after HS/T and the ultimate physiological and biological outcome depends on a balance of these pro- and anti-inflammatory pathways. Further investigation in this area is currently underway.

The mechanisms by which FFP and cryoprecipitate mitigate the EOT are not completely understood. FFP has been shown to decrease shedding of the endothelial glycocalyx, which plays a critical role in the regulation of vascular permeability, microvascular perfusion, and leukocyte and platelet adhesion to the inflamed endothelium.(18-23) Fibrinogen itself may be one key mediator. A recent study showed that plasma but not fibrinogen-deficient plasma reduced permeability of pulmonary endothelial cells *in vitro*.(34) Fibrinogen appears to stabilize endothelial cell surface syndecan-1,(34, 35) which is a key component of the endothelial glycocalyx, and may protect against HS-induced endothelial cell apoptosis.(52) Moreover, there have been hundreds of other proteins identified in FFP outside of clotting factors, many of which have important biologic functions and could potentially mediate some of these protective effects.(53) It is possible that many of these proteins are also present in cryoprecipitate, and we hypothesize that the similar effects we find between FFP and cryoprecipitate are due to these EOT-modulatory proteins common to both products.

One limitation of the current study is that we cannot rule out that the effects of FFP and cryoprecipitate on endothelial permeability and inflammation *in vivo* were due in part to improved blood pressure resulting in a decreased hypoxic insult. Although equal volumes of resuscitative fluid were administered across treatment groups in this study, FFP and cryoprecipitate were superior to LR in restoring MAPs during the 30-minute monitoring period after shock. However, it is important to note that in the past we and others have tested LR at 3X the volume of shed blood in this mouse model of HS/T, which restored MAPs but did not mitigate vascular leak, hence indicating that restoring blood pressures in itself is not enough to mitigate the EOT caused by HS/T.(13, 15, 16) In the current study, rather than using high volumes of crystalloid which are detrimental and now avoided in trauma patients, (12, 54, 55) we instead employed a low-volume resuscitation approach, using only 200 μl of fluid across the treatment groups, which corresponds to one-third to one-fourth of shed blood volume. Another limitation is that we are studying the effects of treatment in an acute 3-hour model of injury, and the differences at later time points may be profoundly different. We do plan to evaluate these treatments in a 24-hour model of HS/T.

In conclusion, this study demonstrates that cryoprecipitate decreases endothelial permeability *in vitro* and *in vivo* and reduces lung injury, inflammation, and vascular instability *in vivo*, similar to FFP. This suggests that the benefits of early administration of cryoprecipitate to trauma patients with hemorrhagic shock may extend beyond improved hemostasis alone through mitigation of the EOT. Future studies should explore the exact mechanisms by which plasma and plasma-derived products protect the injured endothelium in hemorrhagic shock and trauma.

Supplementary Material

Refer to Web version on PubMed Central for supplementary material.

Sources of Funding:

Mark Barry received funding from the National Health Lung and Blood Institute under Award Number R38HL143581. The contents of this research are solely the responsibility of the authors and do not necessarily

represent the official views of the NIH. Funding for these studies was provided by UCSF intramural funds to Shibani Pati.

References

1. Centers for Disease Control and Prevention, National Center for Injury Prevention and Control. Web-based Injury Statistics Query and Reporting System (WISQARS) 2017 [Available from: www.cdc.gov/injury/wisqars.
2. Holcomb JB, Jenkins D, Rhee P, Johannigman J, Mahoney P, Mehta S, Cox ED, Gehrke MJ, Beilman GJ, Schreiber M, et al. Damage control resuscitation: directly addressing the early coagulopathy of trauma. J Trauma. 2007;62(2):307–10. [PubMed: 17297317]
3. Holcomb JB, del Junco DJ, Fox EE, Wade CE, Cohen MJ, Schreiber MA, Alarcon LH, Bai Y, Brasel KJ, Bulger EM, et al. The prospective, observational, multicenter, major trauma transfusion (PROMMTT) study: comparative effectiveness of a time-varying treatment with competing risks. JAMA Surg. 2013;148(2):127–36. [PubMed: 23560283]
4. Holcomb JB, Tilley BC, Baraniuk S, Fox EE, Wade CE, Podbielski JM, del Junco DJ, Brasel KJ, Bulger EM, Callcut RA, et al. Transfusion of plasma, platelets, and red blood cells in a 1:1:1 vs a 1:1:2 ratio and mortality in patients with severe trauma: the PROPPR randomized clinical trial. JAMA. 2015;313(5):471–82. [PubMed: 25647203]
5. Langan NR, Eckert M, Martin MJ. Changing patterns of in-hospital deaths following implementation of damage control resuscitation practices in US forward military treatment facilities. JAMA Surg. 2014;149(9):904–12. [PubMed: 25029432]
6. Cotton BA, Reddy N, Hatch QM, LeFebvre E, Wade CE, Kozar RA, Gill BS, Albarado R, McNutt MK, Holcomb JB. Damage control resuscitation is associated with a reduction in resuscitation volumes and improvement in survival in 390 damage control laparotomy patients. Ann Surg. 2011;254(4):598–605. [PubMed: 21918426]
7. Oyeniyi BT, Fox EE, Scerbo M, Tomasek JS, Wade CE, Holcomb JB. Trends in 1029 trauma deaths at a level 1 trauma center: Impact of a bleeding control bundle of care. Injury. 2017;48(1):5–12. [PubMed: 27847192]
8. Sobrino J, Shafi S. Timing and causes of death after injuries. Proc (Bayl Univ Med Cent). 2013;26(2):120–3. [PubMed: 23543966]
9. Kauvar DS, Wade CE. The epidemiology and modern management of traumatic hemorrhage: US and international perspectives. Crit Care. 2005;9 Suppl 5:S1–9.
10. Acosta JA, Yang JC, Winchell RJ, Simons RK, Fortlage DA, Hollingsworth-Fridlund P, Hoyt DB. Lethal injuries and time to death in a level I trauma center. J Am Coll Surg. 1998;186(5):528–33. [PubMed: 9583692]
11. Jenkins DH, Rappold JF, Badloe JF, Berséus O, Blackbourne L, Brohi KH, Butler FK, Cap AP, Cohen MJ, Davenport R. Trauma hemostasis and oxygenation research position paper on remote damage control resuscitation: definitions, current practice, and knowledge gaps. Shock. 2014;41 Suppl 1:3–12.
12. Holcomb JB, Pati S. Optimal trauma resuscitation with plasma as the primary resuscitative fluid: the surgeon's perspective. Hematology Am Soc Hematol Educ Program. 2013;2013:656–9. [PubMed: 24319247]
13. Peng Z, Pati S, Potter D, Brown R, Holcomb JB, Grill R, Wataha K, Park PW, Xue H, Kozar RA. Fresh frozen plasma lessens pulmonary endothelial inflammation and hyperpermeability after hemorrhagic shock and is associated with loss of syndecan 1. Shock. 2013;40(3):195–202. [PubMed: 23807246]
14. Pati S, Potter DR, Baimukanova G, Farrel DH, Holcomb JB, Schreiber MA. Modulating the endotheliopathy of trauma: Factor concentrate versus fresh frozen plasma. J Trauma Acute Care Surg. 2016;80(4):576–84; discussion 84-5. [PubMed: 26808040]
15. Pati S, Peng Z, Wataha K, Miyazawa B, Potter DR, Kozar RA. Lyophilized plasma attenuates vascular permeability, inflammation and lung injury in hemorrhagic shock. PLoS One. 2018;13(2):e0192363. [PubMed: 29394283]
16. Potter DR, Baimukanova G, Keating SM, Deng X, Chu JA, Gibb SL, Peng Z, Muench MO, Fomin ME, Spinella PC, et al. Fresh frozen plasma and spray-dried plasma mitigate pulmonary vascular

permeability and inflammation in hemorrhagic shock. J Trauma Acute Care Surg. 2015;78(6 Suppl 1):S7–S17. [PubMed: 26002267]

17. Pati S, Matijevic N, Doursout MF, Ko T, Cao Y, Deng X, Kozar RA, Hartwell E, Conyers J, Holcomb JB. Protective effects of fresh frozen plasma on vascular endothelial permeability, coagulation, and resuscitation after hemorrhagic shock are time dependent and diminish between days 0 and 5 after thaw. J Trauma. 2010;69 Suppl 1:S55–63. [PubMed: 20622621]
18. Kozar RA, Pati S. Syndecan-1 restitution by plasma after hemorrhagic shock. J Trauma Acute Care Surg. 2015;78(6 Suppl 1):S83–6. [PubMed: 26002270]
19. Chignalia AZ, Yetimakman F, Christiaans SC, Unal S, Bayrakci B, Wagener BM, Russell RT, Kerby JD, Pittet JF, Dull RO. THE GLYCOCALYX AND TRAUMA: A REVIEW. Shock. 2016;45(4):338–48. [PubMed: 26513707]
20. Milford EM, Reade MC. Resuscitation Fluid Choices to Preserve the Endothelial Glycocalyx. Crit Care. 2019;23(1):77. [PubMed: 30850020]
21. Haywood-Watson RJ, Holcomb JB, Gonzalez EA, Peng Z, Pati S, Park PW, Wang W, Zaske AM, Menge T, Kozar RA. Modulation of syndecan-1 shedding after hemorrhagic shock and resuscitation. PLoS One. 2011;6(8):e23530. [PubMed: 21886795]
22. Kozar RA, Peng Z, Zhang R, Holcomb JB, Pati S, Park P, Ko TC, Paredes A. Plasma restoration of endothelial glycocalyx in a rodent model of hemorrhagic shock. Anesth Analg. 2011;112(6):1289–95. [PubMed: 21346161]
23. Wu F, Chipman A, Pati S, Miyasawa B, Corash L, Kozar RA. Resuscitative Strategies to Modulate the Endotheliopathy of Trauma: From Cell to Patient. Shock. 2020;53(5):575–84. [PubMed: 31090680]
24. Hayakawa M, Gando S, Ono Y, Wada T, Yanagida Y, Sawamura A. Fibrinogen level deteriorates before other routine coagulation parameters and massive transfusion in the early phase of severe trauma: a retrospective observational study. Semin Thromb Hemost. 2015;41(1):35–42. [PubMed: 25590522]
25. Floccard B, Rugeri L, Faure A, Saint Denis M, Boyle EM, Peguet O, Levrat A, Guillaume C, Marcotte G, Vulliez A, et al. Early coagulopathy in trauma patients: an on-scene and hospital admission study. Injury. 2012;43(1):26–32. [PubMed: 21112053]
26. Inaba K, Karamanos E, Lustenberger T, Schöchl H, Shulman I, Nelson J, Rhee P, Talving P, Lam L, Demetriades D. Impact of fibrinogen levels on outcomes after acute injury in patients requiring a massive transfusion. J Am Coll Surg. 2013;216(2):290–7. [PubMed: 23211116]
27. McQuilten ZK, Wood EM, Bailey M, Cameron PA, Cooper DJ. Fibrinogen is an independent predictor of mortality in major trauma patients: A five-year statewide cohort study. Injury. 2017;48(5):1074–81. [PubMed: 28190583]
28. Hayakawa M, Maekawa K, Kushimoto S, Kato H, Sasaki J, Ogura H, Matauoka T, Uejima T, Morimura N, Ishikura H, et al. High D-Dimer Levels Predict a Poor Outcome in Patients with Severe Trauma, Even with High Fibrinogen Levels on Arrival: A Multicenter Retrospective Study. Shock. 2016;45(3):308–14. [PubMed: 26882403]
29. Innerhofer P, Fries D, Mittermayr M, Innerhofer N, von Langen D, Hell T, Gruber G, Schmid S, Friesenecker B, Lorenz IH, et al. Reversal of trauma-induced coagulopathy using first-line coagulation factor concentrates or fresh frozen plasma (RETIC): a single-centre, parallel-group, open-label, randomised trial. Lancet Haematol. 2017;4(6):e258–e71. [PubMed: 28457980]
30. Kozek-Langenecker S, Sørensen B, Hess JR, Spahn DR. Clinical effectiveness of fresh frozen plasma compared with fibrinogen concentrate: a systematic review. Crit Care. 2011;15(5):R239. [PubMed: 21999308]
31. Schöchl H, Nienaber U, Maegele M, Hochleitner G, Primavesi F, Steitz B, Arndt C, Hanke A, Voelckel W, Solomon C. Transfusion in trauma: thromboelastometry-guided coagulation factor concentrate-based therapy versus standard fresh frozen plasma-based therapy. Crit Care. 2011;15(2):R83. [PubMed: 21375741]
32. Curry N, Rourke C, Davenport R, Beer S, Pankhurst L, Deary A, Thomas H, Llewelyn C, Green L, Doughty H, et al. Early cryoprecipitate for major haemorrhage in trauma: a randomised controlled feasibility trial. Br J Anaesth. 2015;115(1):76–83. [PubMed: 25991760]

33. Nascimento B, Callum J, Tien H, Peng H, Rizoli S, Karanicolas P, Alam A, Xiong W, Selby R, Garzon AM, et al. Fibrinogen in the initial resuscitation of severe trauma (FiiRST): a randomized feasibility trial. Br J Anaesth. 2016;117(6):775–82. [PubMed: 27956676]
34. Wu F, Kozar RA. Fibrinogen Protects Against Barrier Dysfunction Through Maintaining Cell Surface Syndecan-1 In Vitro. Shock. 2019;51(6):740–4. [PubMed: 29905671]
35. Wu F, Chipman A, Dong JF, Kozar RA. Fibrinogen Activates PAK1/Cofilin Signaling Pathway to Protect Endothelial Barrier Integrity. Shock. 2020.
36. Chesebro BB, Rahn P, Carles M, Esmon CT, Xu J, Brohi K, Frith D, Pittet JF, Cohen MJ. Increase in activated protein C mediates acute traumatic coagulopathy in mice. Shock. 2009;32(6):659–65. [PubMed: 19333141]
37. Atabai K, Matthay MA. The pulmonary physician in critical care. 5: Acute lung injury and the acute respiratory distress syndrome: definitions and epidemiology. Thorax. 2002;57(5):452–8. [PubMed: 11978926]
38. Vandesompele J, De Preter K, Pattyn F, Poppe B, Van Roy N, De Paepe A, Speleman F. Accurate normalization of real-time quantitative RT-PCR data by geometric averaging of multiple internal control genes. Genome Biol. 2002;3(7):RESEARCH0034. [PubMed: 12184808]
39. Benjamini Y, Yekutieli D. The Control of the False Discovery Rate in Multiple Testing Under Dependency. Ann Stat. 2001;29(4):1165–88.
40. Désirée Boehme J, Pietkiewicz S, Lavrik I, Jeron A, Bruder D. Morphological and Functional Alterations of Alveolar Macrophages in a Murine Model of Chronic Inflammatory Lung Disease. Lung. 2015;193(6):947–53. [PubMed: 26319657]
41. Kato K, Diéguez-Hurtado R, Park DY, Hong SP, Kato-Azuma S, Adams S, Stehling M, Trappmann B, Wrana JL, Koh GY, et al. Pulmonary pericytes regulate lung morphogenesis. Nat Commun. 2018;9(1):2448. [PubMed: 29934496]
42. Simard JC, Cesaro A, Chapeton-Montes J, Tardif M, Antoine F, Girard D, Tessier PA. S100A8 and S100A9 induce cytokine expression and regulate the NLRP3 inflammasome via ROS-dependent activation of NF-κB(1.). PLoS One. 2013;8(8):e72138. [PubMed: 23977231]
43. Vourc'h M, Roquilly A, Asehnoune K. Trauma-Induced Damage-Associated Molecular Patterns-Mediated Remote Organ Injury and Immunosuppression in the Acutely Ill Patient. Front Immunol. 2018;9:1330. [PubMed: 29963048]
44. He Y, Hara H, Núñez G. Mechanism and Regulation of NLRP3 Inflammasome Activation. Trends Biochem Sci. 2016;41(12):1012–21. [PubMed: 27669650]
45. Grailer JJ, Canning BA, Kalbitz M, Haggadone MD, Dhond RM, Andjelkovic AV, Zetoune FS, Ward PA. Critical role for the NLRP3 inflammasome during acute lung injury. J Immunol. 2014;192(12):5974–83. [PubMed: 24795455]
46. Xiang M, Shi X, Li Y, Xu J, Yin L, Xiao G, Scott MJ, Billiar TR, Wilson MA, Fan J. Hemorrhagic shock activation of NLRP3 inflammasome in lung endothelial cells. J Immunol. 2011;187(9):4809–17. [PubMed: 21940680]
47. Xu P, Wen Z, Shi X, Li Y, Fan L, Xiang M, Li A, Scott MJ, Xiao G, Li S, et al. Hemorrhagic shock augments Nlrp3 inflammasome activation in the lung through impaired pyrin induction. J Immunol. 2013;190(10):5247–55. [PubMed: 23585683]
48. Bortolotti P, Faure E, Kipnis E. Inflammasomes in Tissue Damages and Immune Disorders After Trauma. Front Immunol. 2018;9:1900. [PubMed: 30166988]
49. Ichikawa A, Kuba K, Morita M, Chida S, Tezuka H, Hara H, Sasaki T, Ohteki T, Ranieri VM, dos Santos CC, et al. CXCL10-CXCR3 enhances the development of neutrophil-mediated fulminant lung injury of viral and nonviral origin. Am J Respir Crit Care Med. 2013;187(1):65–77. [PubMed: 23144331]
50. Yamasaki S, Ishikawa E, Sakuma M, Hara H, Ogata K, Saito T. Mincle is an ITAM-coupled activating receptor that senses damaged cells. Nat Immunol. 2008;9(10):1179–88. [PubMed: 18776906]
51. Coornaert B, Carpentier I, Beyaert R. A20: central gatekeeper in inflammation and immunity. J Biol Chem. 2009;284(13):8217–21. [PubMed: 19008218]

52. Yu Q, Yang B, Davis JM, Ghosn J, Deng X, Doursout MF, Dong JF, Wang R, Holcomb JB, Wade CE, et al. Identification of Fibrinogen as a Key Anti-Apoptotic Factor in Human Fresh Frozen Plasma for Protecting Endothelial Cells In Vitro. Shock. 2020;53(5):646–52. [PubMed: 31454826]

53. Schenk S, Schoenhals GJ, de Souza G, Mann M. A high confidence, manually validated human blood plasma protein reference set. BMC Med Genomics. 2008;1:41. [PubMed: 18793429]

54. Chang R, Holcomb JB. Optimal Fluid Therapy for Traumatic Hemorrhagic Shock. Crit Care Clin. 2017;33(1):15–36. [PubMed: 27894494]

55. Chatrath V, Khetarpal R, Ahuja J. Fluid management in patients with trauma: Restrictive versus liberal approach. J Anaesthesiol Clin Pharmacol. 2015;31(3):308–16. [PubMed: 26330707]

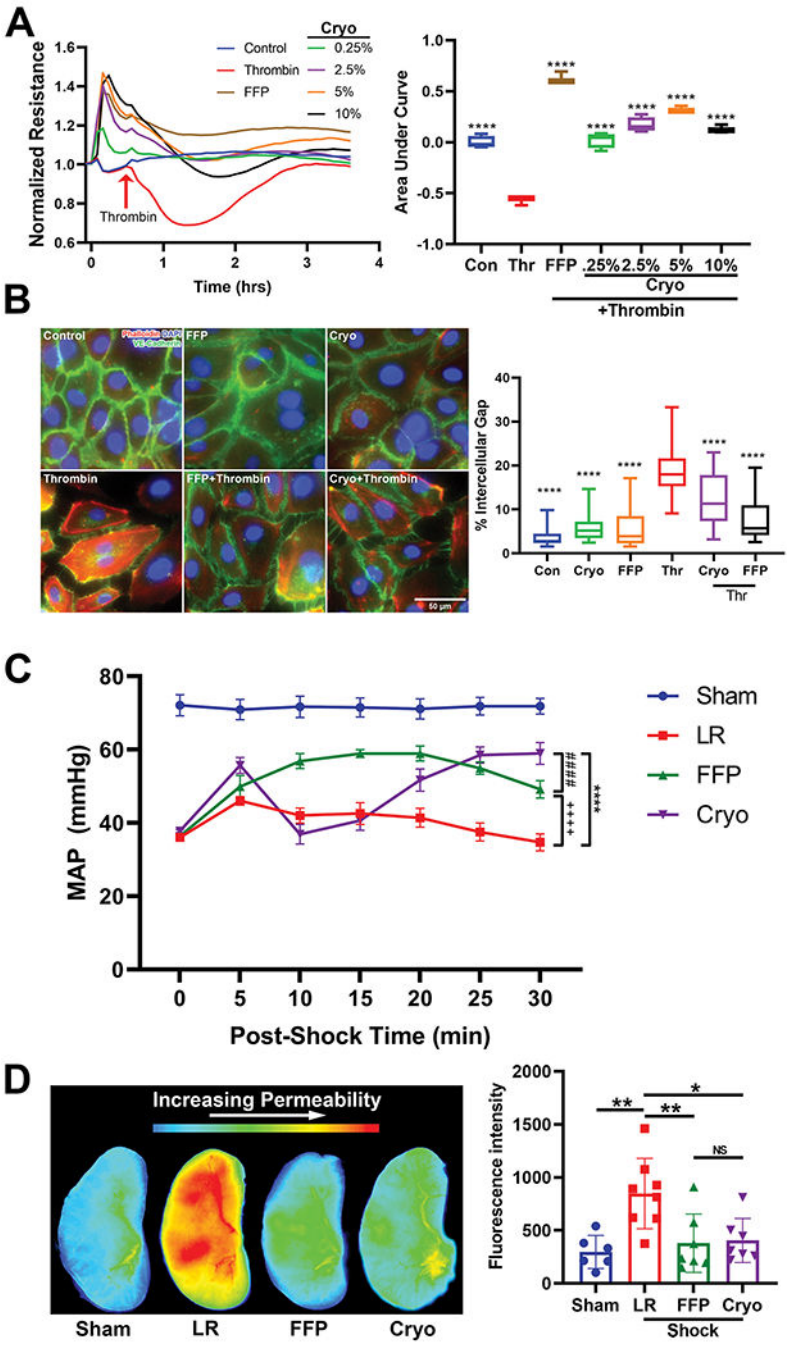

Figure 1. Cryoprecipitate and FFP protect the endothelial barrier *in vitro* against thrombin challenge and reduce vascular permeability *in vivo* in a mouse model of hemorrhagic shock and trauma (HS/T).

(A) Transendothelial electrical resistance (TEER) tracings of human umbilical vein endothelial cells (HUVECs) treated with FFP or cryoprecipitate at different concentrations. Boxplots represent area under the curve quantitation of changes in barrier resistance. ****p<0.0001 vs. thrombin by one-way ANOVA with post-hoc Tukey's tests. N=3-4 cell replicates per treatment. Con=control, Thr=thrombin. (B) Representative images of HUVECs stained for adherens junctions (VE-cadherin, green) and F-actin (Phalloidin, red),

and quantitation of gap formation between ECs. N=25 images per well, 3 wells per condition. ****p<0.0001 vs. thrombin by one-way ANOVA with post-hoc Tukey's tests. (C) Mean arterial pressures (MAPs) in mice subjected to HS/T are presented during the 30 minutes following resuscitation with LR, FFP, or cryoprecipitate. Comparing LR-, FFP-, and cryoprecipitate-treated animals, there was a significant treatment by time interaction with repeated measures two-way ANOVA (p<0.0001). By Tukey's multiple comparisons test, the following comparisons were statistically significant: *cryo vs. FFP* p<0.0001 at 10 and 15 min, p<0.05 at 30 min; *cryo vs. LR* p<0.01 at 5 min, p<0.05 at 20 min, p<0.0001 at 25 and 30 min; *FFP vs. LR* p<0.0001 at 10, 15, 20, and 25 min, p<0.001 at 30 min. N=12-18 mice per group. (D) Representative images of fluorescence intensity in the lung as a measure of pulmonary vascular permeability, and quantitation of fluorescence intensity. Columns indicate mean±SD *p<0.05, **p<0.01 by one-way ANOVA with Tukey's post hoc tests (Sham vs. LR p=0.003, LR vs. FFP p=0.009, LR vs. cryo p=0.01). NS=not significant. N=6-8 mice per group.

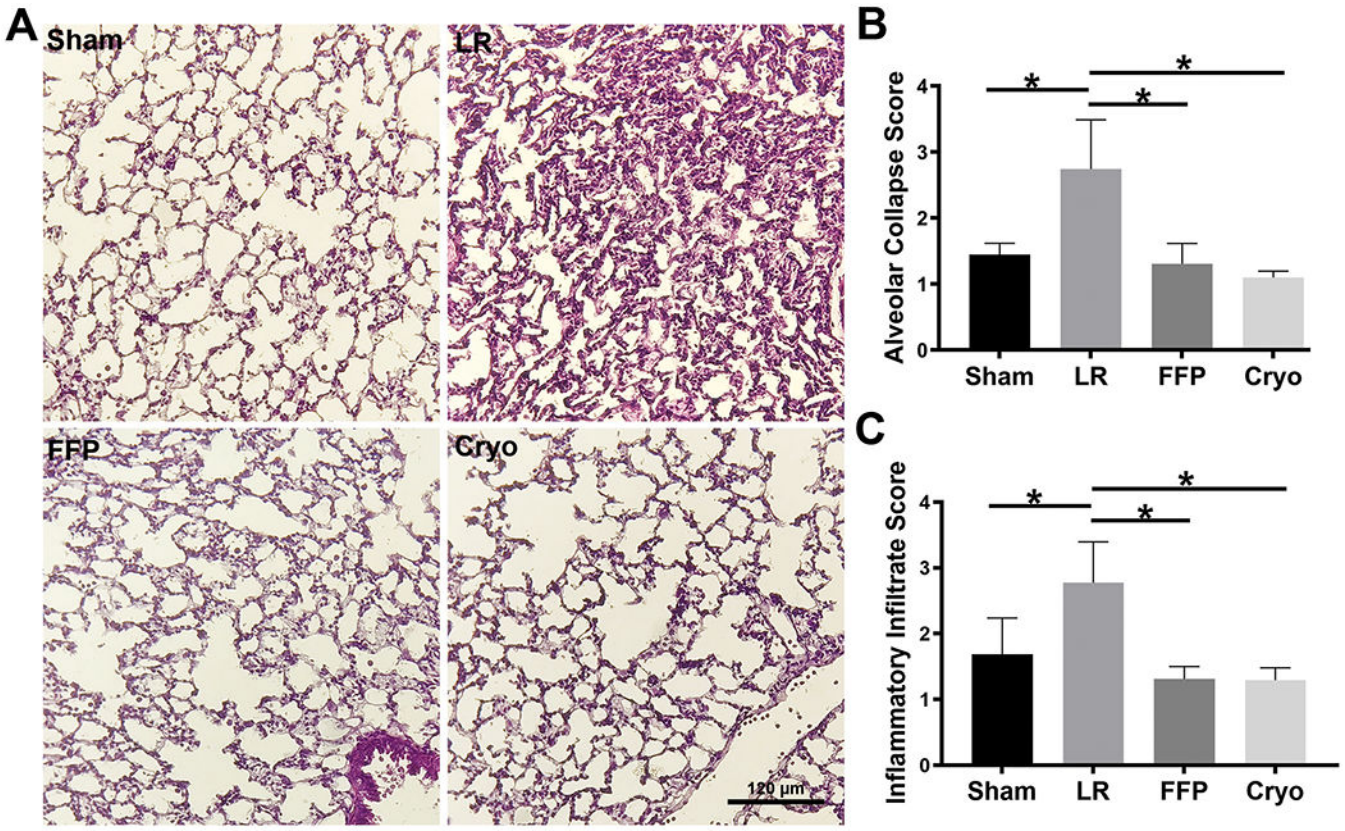

Figure 2. Histopathologic analysis of the lungs after H&E.

(A) Representative images of the lungs from each treatment group showing significant alveolar injury only in the LR-treated mice. (B) Quantitation of alveolar collapse demonstrated significantly reduced injury in HS/T animals treated with FFP or cryoprecipitate compared to those treated with LR. N=4-8 mice per group. *p<0.05 by one-way ANOVA with Tukey's post hoc tests. (C) Quantitation of inflammatory cell infiltrates demonstrated significantly reduced infiltration in HS/T animals treated with FFP or cryoprecipitate compared to those treated with LR. N=4-8 mice per group. *p<0.05 by one-way ANOVA with Tukey's post hoc tests.

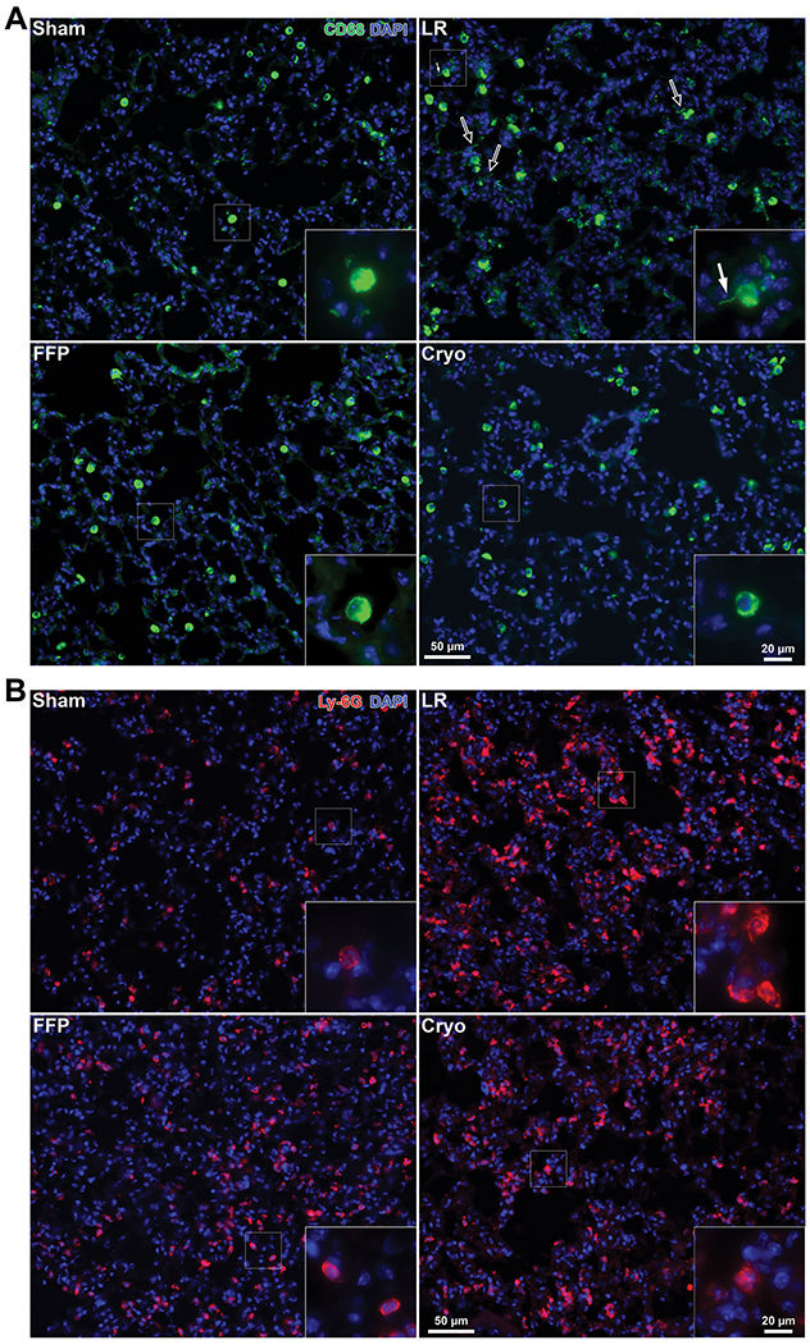

Figure 3. Cryoprecipitate and FFP reduce hemorrhagic shock and trauma (HS/T)-induced activation of macrophages and infiltration of neutrophils.

(A) Representative images stained for CD68 (green), a marker of monocytes and macrophages. HS/T with LR resuscitation is associated with activated alveolar macrophage morphology including increased membrane protrusions (marked by arrows). This was decreased in mice treated with FFP or cryoprecipitate. (B) Lungs stained for Ly6G (red), a marker of neutrophils, demonstrate neutrophil infiltration induced by HS/T in the LR-treated group, which is attenuated in the FFP and cryoprecipitate groups. Nuclei are stained blue with DAPI.

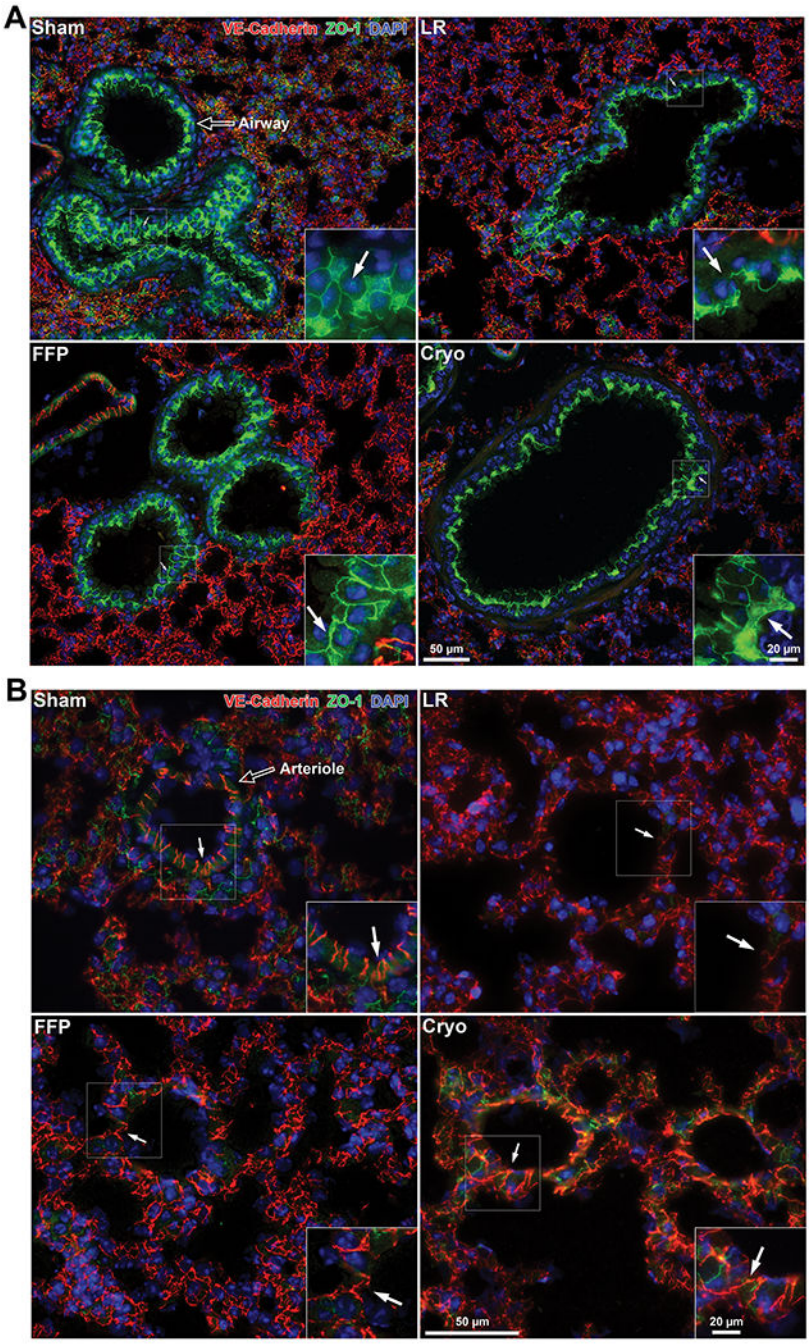

Figure 4. Cryoprecipitate and FFP attenuate the loss of epithelial and endothelial cell junctions induced by hemorrhagic shock and trauma (HS/T).

Representative images of lungs stained for VE-cadherin (endothelial adherens junctions; red), ZO-1 (endothelial and epithelial tight junctions; green), and DAPI (nuclei; blue). (A) HS/T mice treated with LR demonstrate marked loss of ZO-1 staining between epithelial cells (marked by arrows) in the airways compared to sham mice, which is recovered by treatment with FFP and to a lesser extent cryoprecipitate. (B) LR-treated mice demonstrate a loss of staining for VE-cadherin between endothelial cells in small vessels, which is restored by FFP and cryoprecipitate. Arrows point to endothelial junctions.

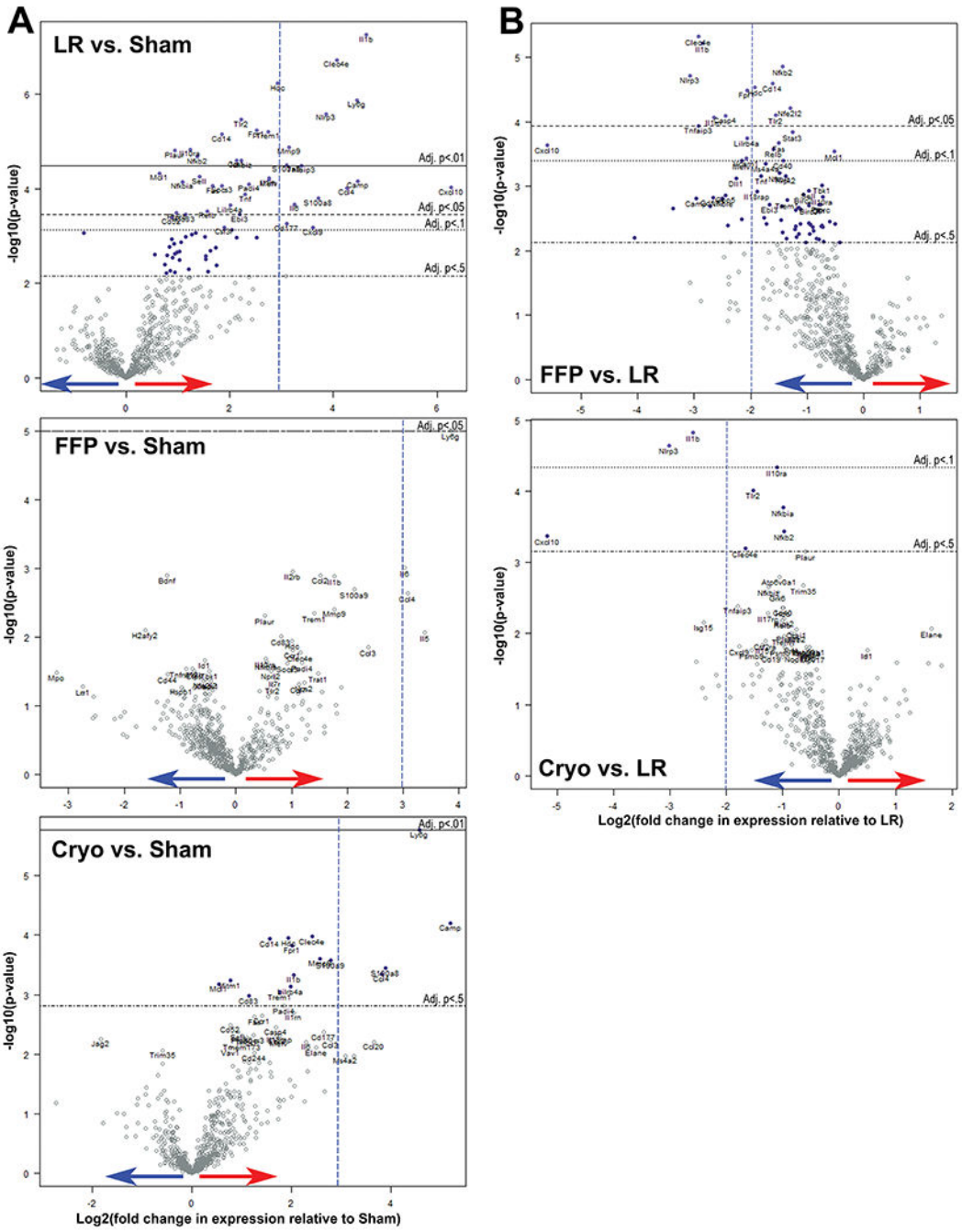

Figure 5. Differential inflammatory gene expression in hemorrhagic shock and trauma (HS/T) analyzed by NanoString.

Volcano plots demonstrate the $\log_2$ fold change in genes compared to sham mice. Values higher on the y-axis have lower p-values, and values farther away from 0 on the x-axis have higher differential expression compared to the baseline group. Red arrow indicates upregulation; blue arrow indicates downregulation. Horizontal lines indicate adjusted p-values by the Benjamini-Yekutieli method. (A) Differential gene expression compared to sham mice. Dashed vertical lines are drawn to orient to a $\log_2$ fold change equal to 3 as the

x-axes differ. (B) Differential gene expression compared to HS/T mice treated with LR. Dashed vertical lines are drawn to orient to a $\log_2$ fold change equal to −2.

Table 1A.

Differential gene expression in HS/T versus sham mice. Genes from the NanoString Mouse Autoimmune Panel with the 40 most statistically significant differences between LR-treated and sham mice are presented here and sorted by $\log_2$ fold change. Animals per group N=3 (sham, FFP, cryoprecipitate) and N=6 (LR). Genes of interest discussed in this paper are highlighted in green. *P-values adjusted by Benjamini-Yekutieli method. **Fold change of CXCL10 is skewed by one LR animal with very high expression of CXCL10; excluding this value results in a $\log_2$ fold change of 3.0 (LR vs. sham).

	Lactated Ringers (LR)			Fresh Frozen Plasma (FFP)			Cryoprecipitate		
Gene	**$\log_2$ Fold Change vs. Sham**	**P**	**Adjusted P***	**$\log_2$ Fold Change vs. Sham**	**P**	**Adjusted P***	**$\log_2$ Fold Change vs. Sham**	**P**	**Adjusted P***
Cxcl10	**6.3****	9.6E-05	0.02	**0.7**	0.60	1	**1.1**	0.39	1
Il1b	**4.6**	5.6E-08	0.0003	**1.8**	0.001	1	**2.0**	0.0005	0.21
Ly6g	**4.5**	1.4E-06	0.002	**3.8**	1.01E-05	0.05	**4.6**	1.7E-06	0.008
Camp	**4.5**	7.0E-05	0.02	**1.5**	0.1	1	**5.2**	6.3E-05	0.11
Ccl4	**4.3**	9.7E-05	0.02	**3.1**	0.0023	1	**3.8**	0.0004	0.21
Clec4e	**4.1**	1.9E-07	0.0005	**1.2**	0.02	1	**2.4**	0.0001	0.11
Nlrp3	**3.9**	2.6E-06	0.003	**0.8**	0.15	1	**0.8**	0.13	1
S100a8	**3.7**	0.0002	0.03	**1.3**	0.12	1	**3.9**	0.0004	0.20
Cxcl9	**3.6**	0.0007	0.08	**0.9**	0.35	1	**1.8**	0.06	1
Tnfaip3	**3.4**	3.3E-05	0.01	**0.5**	0.45	1	**1.6**	0.02	1
Il6	**3.2**	0.0002	0.03	**3.0**	0.001	1	**2.3**	0.006	0.88
Mmp9	**3.1**	1.3E-05	0.006	**1.8**	0.004	1	**2.6**	0.0003	0.16
Cd177	**3.1**	0.0006	0.07	**0.4**	0.57	1	**2.6**	0.004	0.88
S100a9	**3.1**	3.1E-05	0.01	**2.1**	0.002	1	**2.8**	0.0003	0.16
Hdc	**2.9**	5.9E-07	0.001	**1.0**	0.01	1	**1.9**	0.0001	0.11
Il1rn	**2.8**	6.0E-05	0.02	**0.1**	0.83	1	**2.0**	0.0020	0.54
Mefv	**2.8**	6.5E-05	0.02	**0.6**	0.27	1	**1.7**	0.005	0.88
Trem1	**2.7**	6.2E-06	0.004	**1.0**	0.01	1	**1.8**	0.0009	0.30
Fpr1	**2.5**	5.8E-06	0.004	**0.5**	0.23	1	**2.0**	0.0002	0.13
Padi4	**2.4**	8.1E-05	0.02	**1.2**	0.02	1	**1.8**	0.002	0.45
Tnf	**2.3**	0.0001	0.02	**0.5**	0.33	1	**1.3**	0.02	1
Tlr2	**2.2**	3.5E-06	0.003	**0.7**	0.05	1	**0.7**	0.04	1
Nfkbiz	**2.2**	2.6E-05	0.008	**0.7**	0.08	1	**1.0**	0.02	1
Ebi3	**2.2**	0.0004	0.05	**0.5**	0.33	1	**1.7**	0.005	0.88
Ccr1	**2.1**	2.5E-05	0.008	**1.0**	0.02	1	**1.4**	0.002	0.57
Lilrb4a	**2.0**	0.0002	0.04	**−0.1**	0.90	1	**2.0**	0.0007	0.26
Csf3r	**1.9**	0.0007	0.08	**0.8**	0.13	1	**1.2**	0.03	1
Cd14	**1.9**	7.2E-06	0.004	**0.3**	0.39	1	**1.6**	0.0001	0.11
Socs3	**1.8**	8.7E-05	0.02	**0.9**	0.03	1	**1.2**	0.005	0.88
Fas	**1.7**	8.9E-05	0.02	**0.8**	0.49	1	**1.3**	0.002	0.57

	Lactated Ringers (LR)			Fresh Frozen Plasma (FFP)			Cryoprecipitate		
Gene	**Log_2 Fold Change vs. Sham**	**P**	**Adjusted P***	**Log_2 Fold Change vs. Sham**	**P**	**Adjusted P***	**Log_2 Fold Change vs. Sham**	**P**	**Adjusted P***
Relb	**1.6**	0.0003	0.05	**0.0**	0.95	1	**0.6**	0.14	1
Sell	**1.4**	5.6E-05	0.02	**0.4**	0.11	1	**0.9**	0.004	0.88
Nfkb2	**1.4**	2.1E-05	0.008	**−0.1**	0.79	1	**0.4**	0.11	1
Il10ra	**1.2**	1.5E-05	0.006	**0.5**	0.02	1	**0.2**	0.48	1
Cd83	**1.2**	0.0004	0.05	**0.8**	0.01	1	**1.1**	0.001	0.32
Nfkbia	**1.1**	7.1E-05	0.02	**0.5**	0.02	1	**0.1**	0.61	1
Ptprc	**1.0**	0.0003	0.05	**0.2**	0.36	1	**0.4**	0.07	1
Plaur	**0.9**	1.6E-05	0.006	**0.5**	0.005	1	**0.3**	0.04	1
Cd52	**0.9**	0.0004	0.05	**0.4**	0.06	1	**0.8**	0.003	0.75
Mcl1	**0.6**	4.7E-05	0.01	**0.1**	0.30	1	**0.5**	0.0007	0.25

Table 1B.

Differential gene expression in HS/T mice treated with FFP or cryoprecipitate versus LR. Genes from the NanoString Mouse Autoimmune Panel with the 30 most statistically significant differences between FFP- and LR-treated animals are presented here and sorted by $\log_2$ fold change. Animals per group N=3 (FFP, cryoprecipitate) and N=6 (LR). Genes of interest discussed in this paper are highlighted in green. *P-values adjusted by Benjamini-Yekutieli method. **Fold change of CXCL10 is skewed by one LR animal with very high expression of CXCL10; excluding this value results in a $\log_2$ fold change of −2.2 (FFP vs. LR) and −2.1 (cryoprecipitate vs. LR).

	Fresh Frozen Plasma (FFP)			Cryoprecipitate		
Gene	**$\log_2$ Fold Change vs. LR**	**P**	**Adjusted P***	**$\log_2$ Fold Change vs. LR**	**P**	**Adjusted P***
Cxcl10	**−5.6****	0.0002	0.07	**−5.1****	0.0004	0.3
Nlrp3	**−3.1**	1.9E-05	0.02	**−3.0**	2.3E-05	0.06
Clec4e	**−2.9**	4.8E-06	0.02	**−1.7**	0.0006	0.39
Tnfaip3	**−2.9**	0.0001	0.05	**−1.8**	0.004	1
Il1b	**−2.9**	6.1E-06	0.02	**−2.6**	1.5E-05	0.06
Il1rn	**−2.6**	8.6E-05	0.04	**−0.7**	0.13	1
Casp4	**−2.5**	8.0E-05	0.04	**0.2**	0.70	1
Dll1	**−2.3**	0.0008	0.14	**−1.3**	0.02	1
Mefv	**−2.2**	0.0004	0.10	**−1.0**	0.04	1
Vcam1	**−2.1**	0.0004	0.10	**−0.6**	0.16	1
Lilrb4a	**−2.1**	0.0002	0.06	**0.0**	0.97	1
Fpr1	**−2.1**	3.2E-05	0.02	**−0.5**	0.11	1
Hdc	**−1.9**	2.9E-05	0.02	**−1.0**	0.004	1
Il18rap	**−1.9**	0.001	0.21	**−0.3**	0.54	1
Tnf	**−1.8**	0.0007	0.14	**−1.0**	0.022	1
Ms4a4a	**−1.7**	0.0005	0.10	**−0.4**	0.24	1
Cd14	**−1.6**	2.5E-05	0.02	**−0.3**	0.24	1
Relb	**−1.6**	0.0003	0.08	**−1.0**	0.006	1
Tlr2	**−1.6**	8.0E-05	0.04	**−1.5**	9.7E-05	0.12
Fas	**−1.5**	0.0002	0.07	**−0.4**	0.17	1
Nfkbiz	**−1.5**	0.0006	0.14	**−1.2**	0.002	0.92
Nfkb2	**−1.4**	1.4E-05	0.02	**−1.0**	0.0004	0.3
Cd40	**−1.4**	0.0004	0.10	**−1.0**	0.004	1
Ripk2	**−1.4**	0.0007	0.14	**−1.0**	0.006	1
Nfe2l2	**−1.3**	6.1E-05	0.04	**−0.2**	0.35	1
Stat3	**−1.3**	0.0001	0.06	**−0.5**	0.04	1
Sell	**−1.0**	0.001	0.21	**−0.5**	0.05	1
Tbk1	**−0.7**	0.001	0.18	**0.1**	0.55	1
Il10ra	**−0.7**	0.002	0.22	**−1.1**	4.6E-05	0.08
Mcl1	**−0.5**	0.0003	0.08	**−0.1**	0.32	1